

Neutron-deuteron scattering revisited with the EKM chiral nuclear force and the WPCD method

Qing-Yu Zhai,^{1,2} Dan-Yang Pang,¹ Wen-Di Chen,³ O. A. Rubtsova,⁴ Rui-Rui Xu,⁵ Jun-Xu Lu,^{1,*} Haozhao Liang,^{2,6,7,†} and Li-Sheng Geng^{8,1,9,10,11,‡}

¹*School of Physics, Beihang University, Beijing 102206, China*

²*Department of Physics, Graduate School of Science, The University of Tokyo, Tokyo 113-0033, Japan*

³*Institute of Applied Physics and Computational Mathematics, Beijing, 100094, People's Republic of China*

⁴*Skobeltsyn Institute of Nuclear Physics, Moscow State University, 119991 Moscow, Russia*

⁵*China Nuclear Data Center, China Institute of Atomic Energy, Beijing, 102413, China*

⁶*Quark Nuclear Science Institute, The University of Tokyo, Tokyo 113-0033, Japan*

⁷*RIKEN Center for Interdisciplinary Theoretical and Mathematical Sciences, Wako 351-0198, Japan*

⁸*Sino-French Carbon Neutrality Research Center, École Centrale de Pékin/School of General Engineering, Beihang University, Beijing 100191, China*

⁹*Peng Huanwu Collaborative Center for Research and Education, Beihang University, Beijing 100191, China*

¹⁰*Beijing Key Laboratory of Advanced Nuclear Materials and Physics, Beihang University, Beijing 102206, China*

¹¹*Southern Center for Nuclear-Science Theory (SCNT), Institute of Modern Physics, Chinese Academy of Sciences, Huizhou 516000, China*

We revisit the neutron-deuteron scattering using the Wave-Packet Continuum Discretization (WPCD) method with the EKM chiral nuclear force at various chiral orders. We rederive the permutation operator and solve the Faddeev-AGS equations directly, without rewriting the initial Faddeev kernel tG_0 and introducing pseudo-states, thereby rendering the approach easily extendable to a relativistic framework. We find that up to the next-to-next-to-next-to-leading order (N^3LO), although one can well describe the differential cross sections, one cannot resolve the long-standing A_y puzzle, consistent with previous studies. The fact that the N^3LO chiral forces can well describe the NN phase shifts and the results obtained with the EKM and Idaho N^3LO chiral forces agree with each other underscores the need for further investigations to resolve the A_y puzzle, e.g., considering three-body forces or relativistic effects.

I. INTRODUCTION

Neutron-deuteron (nd) scattering is one of the most extensively studied processes in nuclear physics. As a three-body system, it can be solved with *ab-initio* methods, which serve as a standard reference for testing nuclear forces and validating few-body methods.

In 1960, L.D. Faddeev proposed the now well-known Faddeev equations for a rigorous solution of quantum three-body problems [1]. As a set of three integral equations equivalent to the Lippmann-Schwinger equation for two-body systems, the Faddeev equations feature a compact integral kernel composed of two-body t matrices and the three-body Green function. In fact, the Faddeev formalism has been generalized to more than three particles by Yakubovsky [2]. Building on the Faddeev formalism, in 1967, E.O. Alt, P. Grassberger, and W. Sandhas introduced the Alt-Grassberger-Sandhas (AGS) equation, which reformulates the scattering process in terms of transition operators instead of three-body wave functions, thereby simplifying the computation of physical observables. Furthermore, H. Witala et al. developed a method to solve the three-nucleon Faddeev equations including relativistic features, in which the Green functions and permutation operators take relativistic forms and the NN interaction is supplemented by boost corrections [3–5].

In general, the Faddeev-AGS equations are solved in mo-

mentum space, with a systematic method proposed in Ref. [6]. However, in this approach, one must deal with complicated t -matrix interpolations and the moving singularities of the three-body Green function, which has traditionally required the use of supercomputers. Since the t matrices can be obtained analytically with separable potentials, a simplified approach is to approximate the nuclear force by an expansion in separable potentials [7, 8], whereby the Faddeev-AGS equations can be reformulated into quasiparticle equations that are much easier to solve; however, this method is inadequate for accurately treating three-nucleon systems with high-precision nuclear forces. Another perturbative approach for solving the Faddeev-AGS equations was developed in Ref. [9]. By taking into account one part of the interaction exactly and the other part approximately, one can decompose the two-baryon and three-baryon transition matrices into two parts, and then the Faddeev-AGS equations can be solved by iteration. Even so, one still has to deal with the complex numerical computations arising from interpolation and singularities. Recently, O.A. Rubtsova, V.I. Kukulin, and V.N. Pomerantsev developed the Wave-Packet Continuum Discretization (WPCD) method [10]. In this approach, the continuum states of a three-body system are coarse-grained into a square-integrable basis, thereby smoothing out all singularities and facilitating straightforward numerical solutions of the Faddeev-AGS equations. Combined with GPU-based parallel computing, this method enables efficient solution of the equations even on a personal computer [11].

In Ref. [12], the authors systematically investigated the algorithms, convergence, and other related aspects involved in solving the Faddeev-AGS equations with the Idaho next-

* Corresponding author: ljxwohool@buaa.edu.cn

† Corresponding author: haozhao.liang@phys.s.u-tokyo.ac.jp

‡ Corresponding author: lisheng.geng@buaa.edu.cn

to-next-to-next-to-leading order ($N^3\text{LO}$) and chiral optimized next-to-next-to-leading order ($N^2\text{LO}_{\text{opt}}$) interactions using the WPCD method. In contrast, in the present work, we solve the Faddeev-AGS equations with the initial Faddeev kernel tG_0 , thereby avoiding any pseudo-state constructions that rely on the Hamiltonian spectrum and can introduce theoretical inconsistencies in relativistic calculations. In addition, we propose a new equivalent expression for the permutation operators. These two technical alternatives yield the same results as the standard Faddeev calculations in standard nonrelativistic studies but are essential for generalizing to a relativistic framework, which will be the subject of future work.

This work is organized as follows. In Sec. II, we briefly present our new formalism for solving the Faddeev-AGS equations and calculating physical observables. Results and discussions are presented in Sec. III, followed by a summary and outlook in the last section.

II. THEORETICAL FORMALISM

A. Faddeev-AGS equations in momentum space

We consider protons and neutrons as identical particles with isospin $1/2$. Therefore, elastic nd scattering without three-nucleon forces is treated using the AGS equations for three identical particles. Explicitly, the AGS equations of the transition operator U read

$$U = Pv + PtG_0U, \quad (1)$$

where v is the NN interaction, t is the two-body t -matrix defined by the Lippmann-Schwinger equation, $P = P_{12}P_{23} + P_{13}P_{23}$ is the permutation operator, which determines the overlap between different Jacobi channels, and

$$G_0 = \frac{1}{E + i\epsilon - H_0}, \text{ with } H_0 = E_p + E_q \equiv \frac{p^2}{m} + \frac{3q^2}{4m}$$

is the free three-particle propagator, where m is the mass of the nucleon and E is the kinetic energy of the three-body system, p and q denote the standard Jacobi momenta, as illustrated in Fig. 1.

B. Setting up the WPCD basis

We define free wave-packets using plane-wave states $|p\rangle$. Since the plane-wave basis spans an infinite-dimensional Hilbert space, to set up the WPCD method, first we need to choose a momentum cutoff p_{cut} and discretize continuous momenta. From the perspective of effective field theories, we are primarily concerned with the low-energy region, where the momentum grid should be chosen more densely. In this work, we use the Chebyshev grid [10]

$$p_n = p_s \tan\left(\frac{n}{N + N_{\text{add}} + 1} \frac{\pi}{2}\right), \quad n = 0, 1, 2, \dots, N,$$

$$p_s = \frac{p_{\text{cut}}}{\tan\left(\frac{N}{N + N_{\text{add}} + 1} \frac{\pi}{2}\right)},$$

with $p_{\text{cut}} = 4.0$ GeV, $N_{\text{add}} = 2$, and $N = 150$ [12].

Secondly, we define a set of free wave-packets as

$$|p_i\rangle = \frac{1}{N_i} \int_{\mathcal{D}_i} p \, dp \, f(p) |p\rangle,$$

where N_i is the normalization factor and $\mathcal{D}_i \equiv [p_{i-1}, p_i]$. In this work, we use the energy wave-packet, i.e., $f(p) = \sqrt{p}$ and $N_i = \sqrt{p_i^{\text{mid}} \Delta p_i}$, where $\Delta p_i = p_i - p_{i-1}$ and $p_i^{\text{mid}} = (p_i + p_{i-1})/2$. Further details of the WPCD method can be found in Refs. [10, 13].

In this paper, we label the two nucleons in the two-body subsystem as 2 and 3, and the spectator nucleon as 1. We employ the partial-wave (LS) representation,

$$|p_m q_i \gamma\rangle \equiv |p_m q_i (ls) j (js_1) \Sigma (\lambda \Sigma) JM (tt_1) T \tau_T\rangle. \quad (2)$$

where p , l , s , j , and t denote the relative momentum, relative orbital angular momentum, spin, total angular momentum, and isospin of the antisymmetric two-body subsystem (23). The variables q and λ represent the momentum and orbital angular momentum of nucleon 1 relative to the center of mass of nucleons 2 and 3. The “spins” of the two parts (i.e., j and $s_1 = 1/2$) are coupled to form the “total spin” Σ . The total angular momentum and total isospin of the three-body system are J and T , respectively. In this work, we fix $T = 1/2$ and $\tau_T = -1/2$. The momentum-space part of Eq. (2) is the direct product of the wave packets of the two independent Jacobi momenta, which reads

$$|p_m q_i\rangle = \frac{1}{\sqrt{p_m^{\text{mid}} q_i^{\text{mid}} \Delta p_m \Delta q_i}} \int_{\mathcal{D}_{p_m} \mathcal{D}_{q_i}} p \, dp \, q \, dq \, \sqrt{pq} |pq\rangle.$$

C. Computational implementation

Using the basis of Eq. (2), obtaining explicit matrix elements of these operators in the wave-packet representation is not always straightforward. Therefore, we next explain how to calculate the wave-packet matrix elements.

1. G_0 matrix

First, for G_0 , many studies applied elaborate treatments to the moving singularities [6]. However, within the WPCD framework, it suffices to integrate over G_0 alone, which can even be done analytically. In our energy wave-packet basis, it reads

$$\begin{aligned} & \langle p_m q_i \gamma | G_0 | p_n q_j \gamma' \rangle \\ &= \frac{1}{\Delta E_{p_m} \Delta E_{q_i}} [(E - E_{p_m} - E_{q_i}) \log(E - E_{p_m} - E_{q_i}) \\ & \quad - (E - E_{p_m} - E_{q_{i-1}}) \log(E - E_{p_m} - E_{q_{i-1}}) \\ & \quad - (E - E_{p_{m-1}} - E_{q_i}) \log(E - E_{p_{m-1}} - E_{q_i}) \\ & \quad + (E - E_{p_{m-1}} - E_{q_{i-1}}) \log(E - E_{p_{m-1}} - E_{q_{i-1}})], \end{aligned}$$

where $\Delta E_{p_m} = E_{p_m} - E_{p_{m-1}}$, $\Delta E_{q_i} = E_{q_i} - E_{q_{i-1}}$, and $\log(x) = \log(|x|) + i\pi\Theta(-x)$. Note that we have omitted the global δ -functions $\delta_{mn}\delta_{ij}\delta_{\gamma\gamma'}$, which means that G_0 is diagonal.

2. t matrix

Secondly, t has singularities at the deuteron pole [6]

$$\begin{aligned} & \langle p_m q_i \gamma | t | p_n q_j \gamma' \rangle \\ &= \frac{1}{\mathcal{N}} \int p dp p' dp' q dq \sqrt{pp'} t_{\gamma\gamma'} \left(p, p'; E - \frac{3q^2}{4m} \right) \delta_{ij} \\ &= \frac{1}{\mathcal{N}} \int p dp p' dp' dE_q \sqrt{pp'} \frac{\tilde{t}_{\gamma\gamma'}(p, p'; E - E_q)}{E - E_q - E_d + i\epsilon} \delta_{ij}, \end{aligned}$$

where $\gamma^{(i)}$ matches the 3S_1 - 3D_1 channel and $E_d \simeq -2.2245$ MeV is the binding energy of the deuteron. When $E - E_d \in [E_{q_{i-1}}, E_{q_i}]$, the matrix element of t has a non-trivial imaginary part, which originates from the propagating deuteron. In Refs. [10, 12], as well as in many other studies, this difficulty was avoided by using the identity $tG_0 = vG$, where $G = (E + i\epsilon - H_0 - v)^{-1}$. In this way, the t -operator does not appear in the equations, and the scattering wave packets—namely the pseudo-states, which are eigenstates of the Hamiltonian and can be expanded by the free wave packets in the vicinity of their eigenenergies—were introduced to diagonalize G . However, defining a Hamiltonian in a relativistic scheme generally leads to inconsistencies, and the same issue arises when constructing scattering wave packets. This approach is difficult to generalize to the relativistic case. Therefore, we discretize the integration energy E_q along a complex spectator momentum contour (SMC) [14], that is, we use

$$\begin{aligned} \Gamma_{\text{SMC}}(E_q) &= E_q \\ &+ iV_0 \left(1 - e^{(E_{q_{i-1}} - E_q)/w} \right) \left(1 - e^{(E_q - E_{q_i})/w} \right) \end{aligned}$$

where the parameters are set to be $V_0 = w = (E_{q_i} - E_{q_{i-1}})/2$, and $E_q \in [E_{q_{i-1}}, E_{q_i}]$. It is easy to check that the value of the integral along the contour is exactly the complex conjugate of what we need.

3. P matrix

The explicit form of the permutation operator P has been derived in numerous studies on the three-body scattering

equations [6, 12]. Nevertheless, we present here a brief derivation of an equivalent expression for P that allows a straightforward generalization to the relativistic framework and is numerically tractable.

We adopt the following approach to derive the matrix elements of the permutation operator: First, we follow the approach outlined in Ref. [15] and construct the basis of three-body partial wave states with the same coupling orders as Eq. (2). Then, we construct the permutation operator on this basis and follow Refs. [16–18] to calculate their overlap.

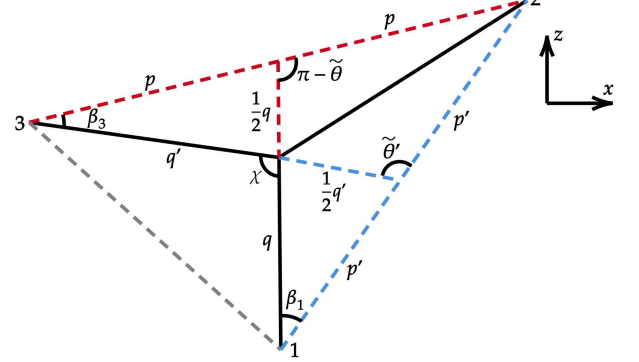


FIG. 1. Momentum assignments of the three nucleons.

Considering the partial-wave basis in Eq. (2), we illustrate the coordinate system and the relative momentum configuration of the three nucleons used in our calculation in Fig. 1, where the momenta p and q follow the definitions in Eq. (2), whereas p' and q' represent the momenta defined in the same way, but for the configuration in which the particle labels have been permuted by $P_{13}P_{23}$. Note that we have omitted the azimuthal angle ϕ of the pair system, as well as the global polar and azimuthal angles Θ and Φ . We denote $S = \{\Phi, \Theta, \phi\}$, which specifies the absolute orientation of the configuration depicted in Fig. 1 within the coordinate system.

We construct the partial-wave basis in Eq. (2) using the helicity basis $|p\lambda\rangle$, which can be easily represented by spinors and exhibits well-behaved transformation properties. We adopt the conventions of Ref. [16]

$$\begin{aligned} \mathcal{U}[L_{-z}(p)]|0-\lambda\rangle &= e^{-i\pi s} \mathcal{U}[R(\pi, \pi, 0)] \mathcal{U}[L_z(p)]|0\lambda\rangle, \\ D_{M, m-\lambda_1}^{J*}(\Phi, \Theta, 0) D_{m, \lambda_2-\lambda_3}^{J*}(\phi, \theta, 0) &\equiv e^{i\lambda_1\phi} D_{M, m-\lambda_1}^{J*}(\Phi, \Theta, \phi) d_{m, \lambda_2-\lambda_3}^J(\theta). \end{aligned}$$

Here, L denotes the transformation of changing the reference

frame of a single particle state, i.e., $L_z(p)|0\lambda\rangle = |p\lambda\rangle$. Ap-

plying these relations, Eq. (2) can then be expanded in the

helicity basis, leading to the explicit expressions

$$\begin{aligned}
& |pq(ls)j(j s_1)\Sigma(\lambda\Sigma)JM(tt_1)T\tau_T\rangle \\
&= \sum_{\substack{m,\lambda_1,\lambda_2,\lambda_3 \\ \tau_1,\tau_2,\tau_3,\tau_t}} \left(\frac{2\lambda+1}{4\pi}\right)^{1/2} \left(\frac{2l+1}{4\pi}\right)^{1/2} \langle t_2\tau_2t_3\tau_3|t\tau_t\rangle \langle t\tau_t t_1\tau_1|T\tau_T\rangle \\
&\quad \times \langle \lambda_0\Sigma m - \lambda_1|Jm - \lambda_1\rangle \langle jm s_1 - \lambda_1|\Sigma m - \lambda_1\rangle \langle l_0s\lambda_2 - \lambda_3|j\lambda_2 - \lambda_3\rangle \langle s_2\lambda_2s_3 - \lambda_3|s\lambda_2 - \lambda_3\rangle \\
&\quad \times \int d\cos\theta dS D_{M,m-\lambda_1}^{J*}(S) d_{m,\lambda_2-\lambda_3}^j(\theta) \mathcal{U}[R(S)] \{e^{-i\pi s_1} \mathcal{U}[R(\pi, \pi, 0)]|q\lambda_1, t_1\tau_1\rangle \\
&\quad \otimes \mathcal{U}[Z(q)]\mathcal{U}[R(0, \theta, 0)]|p\lambda_2, t_2\tau_2\rangle \otimes e^{-i\pi s_3} \mathcal{U}[Z(q)]\mathcal{U}[R(0, \theta, 0)]\mathcal{U}[R(\pi, \pi, 0)]|p\lambda_3, t_3\tau_3\rangle\}, \tag{3}
\end{aligned}$$

where $dS \equiv d\cos\Theta d\Phi d\phi$, $R(S) = e^{-i\Phi J_z} e^{-i\Theta J_y} e^{-i\phi J_z}$, and Z denotes the transformation of changing the reference frame of the pair system along the z -axis. $\mathcal{U}[*]$ denotes the representation of the transformation group.

The representation of P under the basis of Eq. (3) is straightforward. Note that $P_{12}P_{23} = P_{23}P_{13}P_{23}P_{23}$ and $P_{23}^{-1} = P_{23}$, thus

$$\begin{aligned}
& \langle pq(ls)j(j s_1)\Sigma(\lambda\Sigma)JM(tt_1)T\tau_T|P_{23}P_{13}P_{23}P_{23}|p'q'(l's')j'(j's'_1)\Sigma'(\lambda'\Sigma')JM(t't'_1)T\tau_T\rangle \\
&= (-1)^{l+s+t} (-1)^{l'+s'+t'} \langle pq(ls)j(j s_1)\Sigma(\lambda\Sigma)JM(tt_1)T\tau_T|P_{13}P_{23}|p'q'(l's')j'(j's'_1)\Sigma'(\lambda'\Sigma')JM(t't'_1)T\tau_T\rangle
\end{aligned}$$

for nucleons, we have $l + s + t = \text{odd}$, and thus

$\langle p_m q_i \gamma | P_{12} P_{23} | p_n q_j \gamma' \rangle = \langle p_m q_i \gamma | P_{13} P_{23} | p_n q_j \gamma' \rangle$, so we only need to calculate $\langle pq\gamma | P_{13} P_{32} | p'q'\gamma' \rangle$. We have

$$\begin{aligned}
\langle pq\gamma | P_{13} P_{23} | p'q'\gamma' \rangle &= \sum_{hh'} C_{\gamma\gamma'}^{hh'} \int d\cos\theta d\cos\theta' dV D_{m-\lambda_1, m'-\lambda'_3}^{J*}(V) d_{m', \lambda'_1-\lambda'_2}^{j'}(\theta') d_{m, \lambda_2-\lambda_3}^j(\theta) \\
&\quad \times e^{i\pi s_1} \langle q\lambda_1 | \mathcal{U}^{-1}[R(\pi, \pi, 0)] \mathcal{U}[R(V)] \mathcal{U}[Z(q')] \mathcal{U}[R(0, \theta', 0)] | p'\lambda'_1 \rangle \\
&\quad \times e^{-i\pi s_2} \langle p\lambda_2 | \mathcal{U}^{-1}[R(0, \theta, 0)] \mathcal{U}^{-1}[Z(q)] \mathcal{U}[R(V)] \mathcal{U}[Z(q')] \mathcal{U}[R(0, \theta', 0)] \mathcal{U}[R(\pi, \pi, 0)] | p'\lambda'_2 \rangle \\
&\quad \times \langle p\lambda_3 | \mathcal{U}^{-1}[R(\pi, \pi, 0)] \mathcal{U}^{-1}[R(0, \theta, 0)] \mathcal{U}^{-1}[Z(q)] \mathcal{U}[R(V)] \mathcal{U}[R(\pi, \pi, 0)] | q'\lambda'_3 \rangle, \tag{4}
\end{aligned}$$

where $h^{(\prime)} = \{m^{(\prime)}, \lambda_1^{(\prime)}, \lambda_2^{(\prime)}, \lambda_3^{(\prime)}\}$, $R(V) \equiv R(\alpha, \chi, \beta) =$

$R^{-1}(S)R(S')$ denotes the composited rotation, and

$$\begin{aligned}
C_{\gamma\gamma'}^{hh'} &= \frac{1}{2} \frac{(-1)^t}{2J+1} \begin{Bmatrix} t_1 & t_2 & t' \\ t_3 & T & t \end{Bmatrix} \sqrt{(2l+1)(2l'+1)(2\lambda+1)(2\lambda'+1)(2t+1)(2t'+1)} \\
&\quad \times \langle \lambda_0\Sigma m - \lambda_1|Jm - \lambda_1\rangle \langle jm s_1 - \lambda_1|\Sigma m - \lambda_1\rangle \langle l_0s\lambda_2 - \lambda_3|j\lambda_2 - \lambda_3\rangle \langle s_2\lambda_2s_3 - \lambda_3|s\lambda_2 - \lambda_3\rangle \\
&\quad \times \langle \lambda'_0\Sigma' m' - \lambda'_3|Jm' - \lambda'_3\rangle \langle j'm' s_3 - \lambda'_3|\Sigma' m' - \lambda'_3\rangle \langle l'_0s'\lambda'_1 - \lambda'_2|j'\lambda'_1 - \lambda'_2\rangle \langle s_1\lambda'_1s_2 - \lambda'_2|s'\lambda'_1 - \lambda'_2\rangle.
\end{aligned}$$

For further calculation of Eq. (4), in the present non-

relativistic framework, all the $\mathcal{U}[Z(q^{(\prime)})]$ are the representa-

tion of the Galilean transformation, which only changes the momenta, leaving the spinor structure invariant, and the generators of the rotations are

$$J_y = \frac{1}{2} \begin{pmatrix} 0 & i & 0 & 0 \\ -i & 0 & 0 & 0 \\ 0 & 0 & 0 & i \\ 0 & 0 & -i & 0 \end{pmatrix}, \quad J_z = \frac{1}{2} \begin{pmatrix} -1 & 0 & 0 & 0 \\ 0 & 1 & 0 & 0 \\ 0 & 0 & -1 & 0 \\ 0 & 0 & 0 & 1 \end{pmatrix},$$

and the helicity basis

$$|p\lambda\rangle \equiv \begin{pmatrix} 1 \\ 0 \end{pmatrix} \chi_\lambda \otimes |p\rangle, \quad \text{with } \chi_{\frac{1}{2}} = \begin{pmatrix} 1 \\ 0 \end{pmatrix} \text{ and } \chi_{-\frac{1}{2}} = \begin{pmatrix} 0 \\ 1 \end{pmatrix}.$$

According to Fig. 1, we can determine the three remaining angles of rotation V [16], which is $R(V) = R(0, \chi, 0)$. Finally, we arrive at the expression

$$\begin{aligned} & \langle p_m q_i \gamma | P_{13} P_{23} | p_n q_j \gamma' \rangle \\ &= \frac{1}{\sqrt{\Delta p_m \Delta p_n \Delta q_i \Delta q_j}} \sum_{hh'} \int dp dp' dq dq' \frac{(q)^{3/2} (q')^{3/2}}{(p)^{1/2} (p')^{1/2}} \int_0^\pi d\chi \sin \chi C_{\gamma\gamma'}^{hh'} \\ & \times (-1)^{s_1 - \lambda_1 + \lambda_2 + s_2} d_{m-\lambda_1, m' - \lambda'_3}^J(\chi) d_{m, \lambda_2 - \lambda_3}^j(\tilde{\theta}) d_{m', \lambda'_1 - \lambda'_2}^{j'}(\tilde{\theta}') d_{\lambda_1 \lambda'_1}^{s_1}(\beta_1) d_{\lambda_2 \lambda'_2}^{s_2}(\chi - \beta_1 - \beta_3) d_{\lambda_3 \lambda'_3}^{s_3}(-\beta_3) \\ & \times \delta(p - \pi_1) \delta(p' - \pi_3). \end{aligned} \quad (5)$$

where

$$\begin{aligned} \pi_1 &= \sqrt{\frac{1}{4} q^2 + q'^2 + qq' \cos \chi}, \\ \pi_3 &= \sqrt{q^2 + \frac{1}{4} q'^2 + qq' \cos \chi}, \end{aligned}$$

and the angles $\tilde{\theta}$, $\tilde{\theta}'$, β_1 and β_3 can be expressed by the momenta $p^{(i)}$ and $q^{(i)}$ by using the traditional law of cosines. Namely, Eq. (5) is actually a triple integral of $q^{(i)}$ and χ without any singularities. We perform the integration using an 8-point Gaussian quadrature.

D. Spin-scattering matrix and observables

We perform all calculations in the NNN partial wave basis, treating positive and negative parity states separately, with $J \leq 17/2$ and $j \leq 2^1$. This leads to 18 channels for $J = 1/2$, 30 channels for $J = 3/2$, and 34 channels for $J \geq 5/2$, which means that the dimension of the matrices is on the order of several hundred thousand, and direct inversion is impractical. We employ the epsilon algorithm [19] to accelerate the Neumann series of the U -matrix, from which we obtain an approximate convergent value.

In this work, we focus on the differential cross sections and spin observable A_y for elastic nd scattering, which were cal-

culated using the 6×6 spin-scattering matrix \mathcal{M}

$$\begin{aligned} & \mathcal{M}_{m_d m_n, m'_d m'_n}(\theta) \\ &= \frac{2\pi i}{q_0} \sum_{J, P} \sum_{\lambda, \Sigma} \sum_{\substack{m_\Sigma, m_{\Sigma'} \\ \lambda', \Sigma'}} \langle \lambda m_\lambda \Sigma m_\Sigma | JM \rangle \left\langle 1 m_d \frac{1}{2} m_n \middle| \Sigma m_\Sigma \right\rangle \\ & \times \langle \lambda' 0 \Sigma' m_{\Sigma'} | JM \rangle \left\langle 1 m'_d \frac{1}{2} m'_n \middle| \Sigma' m_{\Sigma'} \right\rangle \\ & \times \sqrt{\frac{2\lambda' + 1}{4\pi}} Y_{\lambda m_\lambda}(\theta, 0) \left(S_{\lambda \Sigma, \lambda' \Sigma'}^{JP} - \delta_{\lambda \lambda'} \delta_{\Sigma \Sigma'} \right), \end{aligned}$$

where

$$S_{\lambda \Sigma, \lambda' \Sigma'}^{JP} = \delta_{\lambda \lambda'} \delta_{\Sigma \Sigma'} - i\pi \frac{4}{3} m q_0 U_{\lambda \Sigma, \lambda' \Sigma'}^{JP},$$

and q_0 is the momentum in the c.m.s. of the nd system. We can derive the observables using

$$\begin{aligned} \frac{d\sigma}{d\Omega} &= \frac{1}{6} \text{Tr}(\mathcal{M} \mathcal{M}^\dagger), \\ A_y(n) &= \frac{\text{Tr}(\mathcal{M} \Sigma_y \mathcal{M}^\dagger)}{\text{Tr}(\mathcal{M} \mathcal{M}^\dagger)}, \end{aligned}$$

where $\Sigma_y = \mathbb{I}_{3 \times 3} \otimes \sigma_y$.

III. NUMERICAL RESULTS AND DISCUSSIONS

To verify the validity of our framework, we compute the nd scattering phase shifts for $J^P \leq 7/2^\pm$ at $E_{\text{lab}} = 13$ MeV and the neutron analyzing power $A_y(n)$ at $E_{\text{lab}} = 35$ MeV using the Nijmegen-I and EKM NN interactions, shown in Table I. The results obtained with the Nijmegen-I potential are compared with those from a standard Faddeev calculation reported in Ref. [6], serving as a benchmark. As shown in Table I, our

¹ Note that Ref. [12] used $j \leq 3$, however, it has been proven that $j \leq 2$ is sufficient to obtain accurate elastic scattering observables for $E_{\text{lab}} \lesssim 100$ MeV [6], which is the focus of this work.

TABLE I. Eigen phase shifts and mixing parameters for elastic nd scattering at $E_{\text{lab}} = 13$ MeV. The format is (real part, imaginary part). The Nijm I results in the first column are taken from Ref. [6].

J^P	$\delta_{\Sigma\lambda}$	Nijm I	Nijm I	EKM (N ³ LO)	J^P	$\delta_{\Sigma\lambda}$	Nijm I	Nijm I	EKM (N ³ LO)
$\frac{1}{2}^+$	$\delta_{\frac{3}{2}2}$	(-7.67, 0.57)	(-7.52, 0.58)	(-7.64, 0.57)	$\frac{1}{2}^-$	$\delta_{\frac{1}{2}1}$	(-0.83, 8.22)	(-1.31, 8.20)	(-0.45, 8.61)
	$\delta_{\frac{1}{2}0}$	(-73.03, 18.76)	(-73.65, 18.40)	(-74.21, 18.77)		$\delta_{\frac{3}{2}1}$	(36.73, 3.41)	(37.81, 3.53)	(38.12, 3.68)
	η	(1.10, 0.11)	(1.03, 0.19)	(1.05, 0.09)		ϵ	(22.88, 4.89)	(22.96, 4.73)	(23.10, 5.14)
	ξ	(4.57, -0.11)	(4.70, -0.11)	(4.60, -0.11)		ξ	(-2.24, 4.94)	(-2.13, 5.38)	(-2.46, 4.52)
$\frac{3}{2}^+$	$\delta_{\frac{3}{2}0}$	(75.67, 0.29)	(77.62, 0.62)	(77.49, 0.63)	$\frac{3}{2}^-$	$\delta_{\frac{3}{2}3}$	(2.47, 1.12)	(2.51, 1.19)	(2.42, 1.07)
	$\delta_{\frac{1}{2}2}$	(6.84, 1.56)	(6.93, 1.58)	(6.97, 1.69)		$\delta_{\frac{1}{2}1}$	(4.82, 8.52)	(4.50, 8.46)	(5.46, 9.11)
	$\delta_{\frac{3}{2}2}$	(-8.15, 0.57)	(-8.11, 0.57)	(-8.12, 0.57)		$\delta_{\frac{3}{2}1}$	(30.87, 2.91)	(30.69, 3.03)	(31.50, 3.09)
	η	(-1.67, -0.22)	(-1.76, -0.21)	(-1.67, -0.22)		η	(3.95, -19.65)	(3.53, -20.58)	(4.75, -18.16)
$\frac{5}{2}^+$	ϵ	(2.03, 0.51)	(1.89, 0.54)	(2.06, 0.52)	$\frac{5}{2}^-$	ϵ	(-15.04, -4.42)	(-15.55, -4.53)	(-15.02, -4.83)
	ξ	(4.57, -0.11)	(4.70, -0.11)	(4.60, -0.11)		ξ	(-2.24, 4.94)	(-2.13, 5.38)	(-2.46, 4.52)
	$\delta_{\frac{3}{2}4}$	(-1.00, 0.02)	(-0.99, 0.02)	(-1.00, 0.02)		$\delta_{\frac{3}{2}1}$	(37.55, 2.41)	(37.86, 2.51)	(38.17, 2.53)
	$\delta_{\frac{1}{2}2}$	(6.67, 1.53)	(7.36, 1.36)	(7.41, 1.47)		$\delta_{\frac{1}{2}3}$	(-1.18, 0.22)	(-1.15, 0.22)	(-1.17, 0.24)
$\frac{7}{2}^+$	$\delta_{\frac{3}{2}2}$	(-9.30, 0.58)	(-9.34, 0.58)	(-9.28, 0.59)	$\frac{7}{2}^-$	$\delta_{\frac{3}{2}3}$	(2.99, 0.08)	(3.00, 0.09)	(3.00, 0.09)
	η	(-4.35, 0.72)	(-3.89, 0.48)	(-3.99, 0.56)		η	(-0.71, 0.09)	(-0.67, 0.09)	(-0.70, 0.09)
	ϵ	(-0.62, -0.24)	(-0.38, -0.26)	(-0.47, -0.25)		ϵ	(0.30, 0.44)	(0.51, 0.45)	(0.31, 0.46)
	ξ	(-3.13, -0.11)	(-3.25, -0.12)	(-3.17, -0.12)		ξ	(1.98, -0.03)	(1.89, -0.03)	(2.00, -0.03)
$\frac{7}{2}^+$	$\delta_{\frac{3}{2}2}$	(-7.62, 0.56)	(-7.57, 0.57)	(-7.59, 0.57)	$\frac{7}{2}^-$	$\delta_{\frac{3}{2}5}$	(0.40, 0.01)	(0.41, 0.01)	(0.40, 0.01)
	$\delta_{\frac{1}{2}4}$	(0.61, 0.04)	(0.62, 0.04)	(0.61, 0.04)		$\delta_{\frac{1}{2}3}$	(-1.12, 0.21)	(-1.10, 0.21)	(-1.11, 0.22)
	$\delta_{\frac{3}{2}4}$	(-0.98, 0.02)	(-0.97, 0.02)	(-0.98, 0.02)		$\delta_{\frac{3}{2}3}$	(3.45, 0.08)	(3.44, 0.09)	(3.47, 0.09)
	η	(-2.71, -0.19)	(-2.81, -0.20)	(-2.74, -0.20)		η	(-9.37, -1.38)	(-9.61, -1.42)	(-9.47, -1.48)
$\frac{7}{2}^+$	ϵ	(-0.45, -0.08)	(-0.62, -0.08)	(-0.47, -0.08)	$\frac{7}{2}^-$	ϵ	(0.14, -0.24)	(0.07, -0.24)	(0.14, -0.25)
	ξ	(6.06, 0.35)	(6.29, 0.38)	(6.13, 0.36)		ξ	(-2.22, 0.05)	(-2.15, 0.06)	(-2.24, 0.06)

results are consistent with the standard Faddeev ones. For the eigen phase shifts, we reproduce the standard results with a relative error of approximately 1%. For the mixing parameters, the relative errors are larger while the absolute errors remain reasonable, and the impact on physical observables is limited.

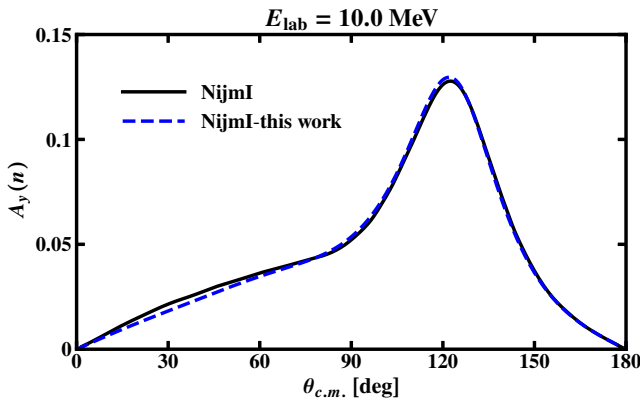


FIG. 2. Neutron analyzing power $A_y(n)$ at $E_{\text{lab}} = 10$ MeV with Nijmegen-I NN interactions. The results denoted by the solid black lines are taken from Ref. [6].

A more straightforward way to benchmark our computation

is by comparing observables. In Fig. 2, we compare with the results from Ref. [12] of the neutron analyzing power $A_y(n)$ at $E_{\text{lab}} = 10$ MeV using the Nijmegen-I NN potential. The perfect agreement verifies our approach is consistent with the standard method. Here, we would like to stress that our approach can be easily modified to suit the relativistic chiral forces recently developed [20, 21].

We also studied the differential cross sections $d\sigma/d\Omega$ and the neutron analyzing power A_y in the region $E_{\text{lab}} \lesssim 50$ MeV with the EKM NN interaction of different chiral orders, the results of which are shown in Fig. 3. Inspection of Fig. 3 indicates that the EKM-N³LO interaction reproduces the data reasonably well, with deviations in A_y around $\theta_{c.m.} \simeq 120^\circ$ only for $E_{\text{lab}} \lesssim 53$ MeV, known as the A_y puzzle. For the differential cross sections, different orders exhibit clear convergence, and even the lowest order provides a satisfactory description in the angular range $90^\circ \lesssim \theta \lesssim 180^\circ$. In contrast, the differential cross section at small angles is more sensitive to the fine details of the nuclear force. For the neutron analyzing power, variations of different orders are strong; the lowest-order term fails to reproduce even the sign of the peak in the experimental data. On the other hand, although EKM-NLO gives a better description than EKM-N³LO, it cannot give a reasonable description of the NN phase shifts, thus it is not a resolution of the A_y puzzle but an alternative wording of the A_y puzzle.

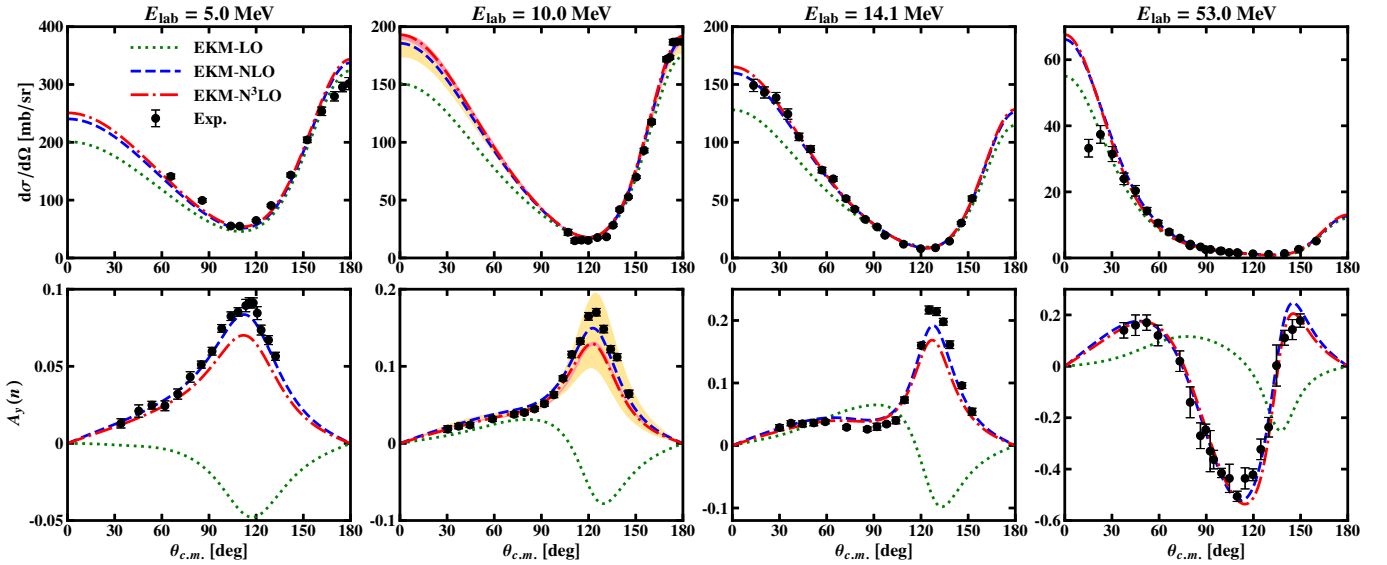


FIG. 3. Differential cross sections $d\sigma/d\Omega$ and the neutron analyzing powers $A_y(n)$ for elastic nd scattering obtained with different chiral orders of the EKM NN interaction. The experimental data at $E_{\text{lab}} = 5$ and 10 MeV are taken from the EXFOR database [22], while the data at $E_{\text{lab}} = 14.1$ and 53 MeV are taken from Refs. [23–25]. The yellow and red bands at $E_{\text{lab}} = 10$ MeV are taken from Ref. [26], which show the estimated theoretical uncertainties at NLO and $N^3\text{LO}$, respectively.

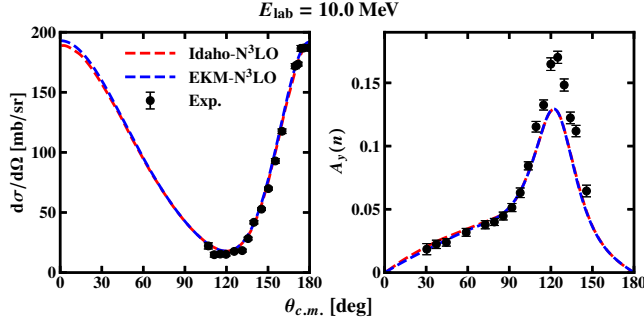


FIG. 4. Differential cross section $d\sigma/d\Omega$ and neutron analyzing power $A_y(n)$ at $E_{\text{lab}} = 10$ MeV with two $N^3\text{LO}$ chiral NN interactions. The results of Idaho- $N^3\text{LO}$ are taken from Ref. [12], and the experimental data are taken from the EXFOR database [22].

In Fig. 4, we show the differential cross sections $d\sigma/d\Omega$ and neutron analyzing power $A_y(n)$ at $E_{\text{lab}} = 10$ MeV with the $N^3\text{LO}$ EKM and Idaho chiral NN interactions. Both potentials produce essentially identical results, consistent with the fact that they can generate nearly the same NN phase shifts—particularly the 3P_j phases, which have a pronounced influence on A_y [6]. It is important to note that neither can reproduce the neutron analyzing power, hinting at the persistent A_y puzzle, which cannot be resolved even with high-precision chiral nuclear forces, consistent with previous studies [26].

IV. SUMMARY AND OUTLOOK

In this work, we proposed a framework for solving the Faddeev-AGS equations using the WPCD method. While

following an approach similar to Refs. [10, 12], our study solved the Faddeev-AGS equations with the EKM chiral nuclear force directly, without introducing pseudo-states, and we presented a new equivalent expression for the permutation operator. With the two improvements above, we showed that our present framework can reproduce the results of the standard Faddeev calculation and allow a straightforward generalization to the relativistic scheme. Furthermore, we studied the differential cross sections $d\sigma/d\Omega$ in the region $E_{\text{lab}} \lesssim 50$ MeV with the EKM NN interaction of different chiral orders and found a good reproduction of the experimental data.

We also studied the neutron analyzing power $A_y(n)$. It was unsurprising that the A_y puzzle emerged once again. Actually, this puzzle has been unresolved for over 30 years. Standard Faddeev calculations have been performed using various NN interactions, and it has been shown that the theory underestimates the data by about 30% [6]. It was once believed that the two-nucleon force based on chiral effective field theory (ChEFT) could resolve this puzzle; however, it persisted [27]. Three-nucleon forces (3NFs) derived consistently in the framework of ChEFT have also been added to the calculation. However, it was found that adding the full $N^3\text{LO}$ 3NF does not improve the description of A_y [28]. Moreover, the $N^3\text{LO}$ 3NFs currently in use are all regularized by a multiplicative regulator applied to the 3NF expressions that are derived from dimensional regularization, which leads to a violation of chiral symmetry at $N^3\text{LO}$ and destroys the consistency between two- and three-nucleon forces [29]. It should be noted that the recently developed relativistic chiral nuclear force [20, 21] incorporates relativistic effects in a self-consistent manner and shows satisfactory convergence. It may provide new insights into this puzzle by enabling a fully rel-

ativistic study of neutron–deuteron scattering. One may expect that relativistic effects could improve the description of A_y , or that the puzzle might be resolved by including only the LO three-body contact terms in the relativistic power counting [30].

V. ACKNOWLEDGMENTS

Qing-Yu Zhai thanks Wei-Jia Kong for the useful discussions. This work is partly supported by the National Natural Science Foundation of China under Grant Nos. 12435007 and 1252200936.

-
- [1] L. D. Faddeev, *Sov. Phys. JETP* **12**, 1014 (1961).
 - [2] O. A. Yakubovsky, *Sov. J. Nucl. Phys.* **5**, 937 (1967).
 - [3] H. Witala, J. Golak, W. Glockle, and H. Kamada, *Phys. Rev. C* **71**, 054001 (2005), arXiv:nucl-th/0412063.
 - [4] H. Witala, J. Golak, R. Skibinski, W. Glockle, W. N. Polyzou, and H. Kamada, *Phys. Rev. C* **77**, 034004 (2008), arXiv:0801.0367 [nucl-th].
 - [5] H. Witala, J. Golak, R. Skibinski, W. Glockle, H. Kamada, and W. N. Polyzou, *Phys. Rev. C* **83**, 044001 (2011), [Erratum: *Phys. Rev. C* **88**, 069904 (2013)], arXiv:1101.4053 [nucl-th].
 - [6] W. Glockle, H. Witala, D. Huber, H. Kamada, and J. Golak, *Phys. Rept.* **274**, 107 (1996).
 - [7] D. J. Ernst, C. M. Shakin, and R. M. Thaler, *Phys. Rev. C* **8**, 46 (1973).
 - [8] D. J. Ernst, C. M. Shakin, and R. M. Thaler, *Phys. Rev. C* **9**, 1780 (1974).
 - [9] A. Deltuva, K. Chmielewski, and P. U. Sauer, *Phys. Rev. C* **67**, 054004 (2003).
 - [10] O. A. Rubtsova, V. I. Kukulin, and V. N. Pomerantsev, *Annals Phys.* **360**, 613 (2015), arXiv:1501.02531 [nucl-th].
 - [11] V. Pomerantsev, V. Kukulin, O. Rubtsova, and S. Sakhiev, *Computer Physics Communications* **204**, 121 (2016).
 - [12] S. B. S. Miller, A. Ekström, and K. Hebeler, *Phys. Rev. C* **106**, 024001 (2022), arXiv:2201.09600 [nucl-th].
 - [13] S. B. S. Miller, A. Ekström, and C. Forssén, *J. Phys. G* **49**, 024001 (2022), arXiv:2106.00454 [nucl-th].
 - [14] Y. Feng, F. Gil, M. Döring, R. Molina, M. Mai, V. Shastri, and A. Szczepaniak, *Phys. Rev. D* **110**, 094002 (2024), arXiv:2407.08721 [nucl-th].
 - [15] S. U. Chung, *Spin formalisms*, CERN Academic Training Lecture (CERN, Geneva, 1971) cERN, Geneva, 1969 - 1970.
 - [16] A. Stadler, F. Gross, and M. Frank, *Phys. Rev. C* **56**, 2396 (1997), arXiv:nucl-th/9703043.
 - [17] G. C. Wick, *Annals Phys.* **18**, 65 (1962).
 - [18] A. McKerrell, *Il Nuovo Cimento* **34**, 1289 (1964).
 - [19] P. Graves-Morris, D. Roberts, and A. Salam, *Journal of Computational and Applied Mathematics* **122**, 51 (2000), *numerical Analysis in the 20th Century Vol. II: Interpolation and Extrapolation*.
 - [20] J.-X. Lu, C.-X. Wang, Y. Xiao, L.-S. Geng, J. Meng, and P. Ring, *Phys. Rev. Lett.* **128**, 142002 (2022), arXiv:2111.07766 [nucl-th].
 - [21] J.-X. Lu, Y. Xiao, Z.-W. Liu, and L.-S. Geng, *Int. J. Mod. Phys. E* **34**, 2543007 (2025), arXiv:2501.17185 [nucl-th].
 - [22] N. Otuka *et al.*, *Nucl. Data Sheets* **120**, 272 (2014), arXiv:2002.07114 [nucl-ex].
 - [23] A. C. Berick, R. A. J. Riddle, and C. M. York, *Phys. Rev.* **174**, 1105 (1968).
 - [24] J. L. Romero *et al.*, *Phys. Rev. C* **25**, 2214 (1982).
 - [25] J. W. Watson, R. Garrett, F. P. Brady, D. H. Fitzgerald, J. L. Romero, J. L. Ullmann, and C. I. Zanelli, *Phys. Rev. C* **25**, 2219 (1982).
 - [26] S. Binder *et al.* (LENPIC), *Phys. Rev. C* **93**, 044002 (2016), arXiv:1505.07218 [nucl-th].
 - [27] D. R. Entem, R. Machleidt, and H. Witala, *Phys. Rev. C* **65**, 064005 (2002), arXiv:nucl-th/0111033.
 - [28] J. Golak *et al.*, *Eur. Phys. J. A* **50**, 177 (2014), arXiv:1410.0756 [nucl-th].
 - [29] E. Epelbaum, H. Krebs, and P. Reinert, *Front. in Phys.* **8**, 98 (2020), arXiv:1911.11875 [nucl-th].
 - [30] L. Girlanda, A. Kievsky, M. Viviani, and L. E. Marcucci, *Phys. Rev. C* **99**, 054003 (2019), arXiv:1811.09398 [nucl-th].